fractal and fractional

MDPI

Article

On Some Novel Soliton Structures for the Beta-Time Fractional Benjamin–Ono Dynamical Equation in Fluids

Mohammed Ahmed Alomair [1] and Kalim U. Tariq [2,*]

[1] Department of Quantitative Methods, School of Business, King Faisal University, Al-Ahsa 31982, Saudi Arabia; ma.alomair@kfu.edu.sa
[2] Department of Mathematics, Mirpur University of Science and Technology (MUST), Mirpur AJK-10250, Pakistan
* Correspondence: kalimulhaq@must.edu.pk

Abstract: This paper consists of an exploration of the wave structures of the Benjamin–Ono equation along with a β-time fractional derivative. The model concerned is utilized to demonstrate internal waves of deep-stratified fluids. Bright, rational, periodic, and many more kinds of solutions for waves are achieved by utilizing the extended sinh-Gordon equation expansion (EShGEE) technique and the improved G'/G-expansion scheme. An influence of fractional-order derivatives was also explored which gives the non-existing results. The Mathematica tool is utilized to gain and verify the results. The results are represented by 3-D, 2-D, and contour graphs. A stability analysis is utilized to confirm that results are precise as well as exact. Modulation instability (MI) is also performed for the steady-state solutions to the concerned model.

Keywords: nonlinear Benjamin–Ono equation; fractional derivative; dynamical analysis; analytical methods; exact solitons; stability analysis; modulation instability analysis

check for updates

Academic Editors: Naben Parumasur, Vijay Kumar Kukreja and Pravin Singh

Received: 5 February 2025
Revised: 13 March 2025
Accepted: 14 March 2025
Published: 17 March 2025

Citation: Alomair, M.A.; Tariq, K.U. On Some Novel Soliton Structures for the Beta-Time Fractional Benjamin–Ono Dynamical Equation in Fluids. *Fractal Fract.* **2025**, *9*, 185. https://doi.org/10.3390/fractalfract9030185

Copyright: © 2025 by the authors. Licensee MDPI, Basel, Switzerland. This article is an open access article distributed under the terms and conditions of the Creative Commons Attribution (CC BY) license (https://creativecommons.org/licenses/by/4.0/).

1. Introduction

Many naturally occurring phenomena are expressed as mathematical models. Many models are constructed as a shape of partial fractional differential equations (FPDEs) in various areas of engineering as well as science, for instance, the fractional paraxial Schrödinger equation [1], fractional Westervelt equation [2], and many others. Fractional calculus plays a significant role across various domains of science and engineering. Different methods have been introduced, including the generalized Riccati expansion technique [3], the Khater II scheme [4], the $(G'/G, 1/G)$-expansion approach [5], and the modified sub-ODE technique [6], among others.

In this research work, the authors utilized two useful and reliable techniques: the EShGEE and the improved (G'/G)-expansion methods. The techniques concerned are utilized for various equations. For example, the extended ShGEE scheme is utilized for the generalized nonlinear Schrödinger model [7], the Kundu–Eckhaus model [8], the Schrödinger model along anti-cubic non-linearity [9], and the generalized Bretherton model [10]. In the same way, the improved (G'/G)-expansion approach is applied to the breaking soliton model [11], the Kaup–Kupershmidt model [12], the modified Kawahara model [13], the Estevez–Mansfield–Clarkson model [14], and many more.

The aim of our research is to discover the distinct results of the fractional Benjamin–Ono model. Furthermore, dynamical analysis is discussed in the form of stability as well as MI analysis.

The motivation of our research is to explore the novel types of wave structures of the Benjamin–Ono model in relation to a β-time fractional derivative. The use of a fractional derivative represents the model in a more prominent form as well as providing more accurate results than the ordinary derivative. The techniques used provide different types of soliton solutions without any limitations/assumptions. Moreover, stability analysis and modulation instability analysis provide us with the stability as well as the accuracy of the solutions and model. The obtained solutions are useful in fluid dynamics and mathematical physics to study wave interaction, wave pattern, wave breaking, ocean engineering, etc.

The rest of the paper is structured as follows. The fractional calculus is introduced in Section 2, while the governing model is shown in Section 3. The analytical strategies are described in Section 4, the scientific computations are carried out in Section 5, the stability process is performed in Section 6, the MI analysis is performed in Section 7, graphical explanations are explored in Section 8, results and discussion are given in Section 9, and we conclude in Section 10.

2. The β-Time Fractional Derivative

The fractional derivative denotes global connectivity compared to the integer order derivative, suggesting that it could represent the dynamic processes involved in function evolution more precisely. In contrast to traditional calculus, which only examines the problem as it stands, mathematical modeling of these situations uses a fractional derivative, which explains why the models are nonlocal. Many researchers have recently examined many types of conformable fractional derivatives that describe various applications [15]. Fractional Taylor power series expansions, the chain rule, Linear differential systems, Laplace transforms, integration by parts, and Gronwall's inequality were some of the concepts that Abdeljawad worked on [16]. Numerous significant physical mechanisms have been described in the literature using a range of fractional derivatives [17]. These include the Atangana [18], the Caputo [19], the modified Riemann–Liouville given by Jumarie [20], and the Beta derivative [21].

Suppose that $v(t)$ is defined $\forall\ t \geq 0$. Therefore, the β-time fractional derivative of v with order Δ is given in [22].

$$D^{\Delta}(v(y)) = \frac{d^{\Delta}v(y)}{dt^{\Delta}} = \lim_{\epsilon \to 0} \frac{v(y + \epsilon(y + \frac{1}{\Gamma(\Delta)})^{1-\Delta}) - v(y)}{\epsilon}, \ \ 0 < \Delta \leq 1.$$

Suppose that $v(y)$ and $u(y)$ are Δ-time differential functions $\forall\ \ y > 0$ and $\Delta \in (0, 1]$, then the given properties are fulfilled [23,24]:

$$\begin{aligned} D^{\Delta}(av(y) + bu(y)) &= aD^{\Delta}(v(y)) + bD^{\Delta}(u(y)), \forall a, b \in \Re. \\ D^{\Delta}(v(y)u(y)) &= u(y)D^{\Delta}(v(y)) + v(y)D^{\Delta}(u(y)), \\ D^{\Delta}(\frac{v(y)}{u(y)}) &= \frac{u(y)D^{\Delta}(v(y)) - v(y)D^{\Delta}(u(y))}{(u(y))^2}, \\ D^{\Delta}(v(y)) &= \left(y + \frac{1}{\Gamma(\Delta)}\right)^{1-\Delta} \frac{dv(y)}{d\Delta}. \end{aligned}$$

3. The Governing Model Presentation

Consider a (1+1)-dimensional non-linear Benjamin–Ono (BO) model given as [25]

$$v_t + \mu v_{xx} + vv_x = 0, \tag{1}$$

$v = v(x, t)$ indicates the wave profile of spatial variablex and temporal variable t. The parameter μ denotes the Hilbert transform operator, which is given as $\mu = \frac{p.v}{\pi}.\int_{-\infty}^{\infty} \frac{\tau(y)}{y-\chi} dy$.

Equation (1) was initially proposed by Benjamin and Ono to describe the internal waves of deep-stratified fluids. In ocean engineering, the fractional Benjamin–Ono equation is usually utilized in computer simulation for the water waves in deep water and open seas [26]. Different types of techniques are applied to determine the various exact solitons including the extended truncated expansion technique [25], the Jacobi elliptic expansion function scheme [26], the new generalized (G'/G)-expansion technique [27], the $\exp(-\phi(\zeta))$-expansion technique [28], (G'/G^2)-expansion method [29], and many others.

The (1+1)-dimensional non-linear Benjamin–Ono model in β-time fractional derivative, which describes the internal single wave event in the atmosphere or water [30], is shown as

$$\frac{\partial^{\Delta} v}{\partial t^{\Delta}} + \mu \frac{\partial^{2\Delta} v}{\partial x^{2\Delta}} + v \frac{\partial^{\Delta} v}{\partial x^{\Delta}} = 0. \tag{2}$$

In the literature, different researchers have discussed the concerned equation; for example, F. Alizadeh et al. adopted the lie symmetries [31], while B. Sagar and S. Saha Ray implemented the unity method [32], whereas B. Babajanov applied the functional variable method [33] and H. Yang et al. employed the multi-scale analysis and perturbation approach [34] to analyse the higher dimensional fractional model efficiently.

4. Methodology

4.1. The Extended ShGEE Technique

In this subsection, we outline the basic points for the technique concerned.

Stage 1:

Consider a non-linear FPDE:

$$Z(g, D_t^{\Delta} g^2, g^2 g_x, g_x, \cdots) = 0 \tag{3}$$

Here, g denotes wave-function. Suppose the following

$$g(x,t) = G(\mho), \ \ \mho = x + \frac{\kappa}{\Delta}(t + \frac{1}{\Gamma(\Delta)})^{\Delta}. \tag{4}$$

Inserting Equation (4) in Equation (3) yields

$$H(G, G^2 G', G'', \cdots) = 0. \tag{5}$$

Stage 2:

Assuming the solutions of Equation (5) given below,

$$G(p) = \alpha_0 + \sum_{j=1}^{m} (\beta_j \sinh(p) + \alpha_j \cosh(p))^j, \tag{6}$$

here, α_0, α_j, β_j $(j = 1, 2, 3, ..., m)$ denote the undetermined. Considering a new profile p of $\mho$ fulfills

$$\frac{dp}{d\mho} = \sinh(p). \tag{7}$$

A positive integer m is calculated by using the homogenous balance (HB) technique. Equation (7) is achieved from the equation below:

$$q_{xt} = \kappa \sinh(v). \tag{8}$$

From [35], one obtains the results for Equation (8), providing

$$\sinh p(\mho) = \pm \operatorname{csc} h(\mho) \text{or} \cosh p(\mho) = \pm \coth(\mho), \tag{9}$$

and

$$sinhp(\mho) = \pm\iota sech(\mho) \text{or} \cosh p(\mho) = \pm \tanh(\mho). \tag{10}$$

$\iota^2 = -1$.

Stage 3:

Using Equation (6) along with Equation (7) in Equation (5), results a set containing $p^{'a}(\mho)\sinh^b p(\mho)\cosh^n p(\mho)$ $(a = 0, 1;\ b = 0, 1;\ n = 0, 1, 2, ...)$. Setting every coefficient of $p^{'a}(\mho)\sinh^b p(\mho)\cosh^n p(\mho)$ equal to zero achieves a set.

Stage 4:

After simplifying the gained set, we achieved the solutions for the undetermined. Using the achieved results, Equations (9) and (10) provide the results of Equation (5), given as

$$G(\mho) = \alpha_0 + \sum_{j=1}^{m}(\pm\beta_j \operatorname{csc} h(\mho) \pm \alpha_j \coth(\mho))^j \tag{11}$$

and

$$G(\mho) = \alpha_0 + \sum_{j=1}^{m}(\pm\iota\beta_j sech(\mho) \pm \alpha_j \tanh(\mho))^j. \tag{12}$$

With the use of this technique, we gain solutions consisting of sech, csc h, tanh, and coth.

4.2. Improved (G'/G)-Expansion Technique

This subsection consists on the basic concept of the scheme [36].

Stage 1: Consider a non-linear PFDE.

$$Z(g, D_t^{\Delta}g, g^2 g_x, ...) = 0. \tag{13}$$

Stage 2: Assume the given transformation:

$$g(x,t) = G(\eta),\ \ \eta = x - \frac{\kappa}{\Delta}(t + \frac{1}{\Gamma(\Delta)})^{\Delta}. \tag{14}$$

where κ denotes the constant. Inserting Equation (14) in Equation (13) provides

$$Y(G, G^2 G^{'}, ...) = 0. \tag{15}$$

Stage 3: Assume the following solution of Equation (15):

$$Q(\eta) = \sum_{i=0}^{m}\alpha_i\left(\frac{G'(\eta)}{G(\eta)}\right)^i. \tag{16}$$

In Equation (16), $\alpha_i, (i = 0, 1, ..., m)$ denote the undetermined. By utilizing the HB approach for Equation (15), we achieve m. A profile $G = G(\eta)$ satisfies the equation:

$$GG'' - \kappa_1 G^2 - \kappa_2 GG' - \kappa_3 (G')^2 = 0, \tag{17}$$

Here, κ_1, κ_2, and κ_3 denote the constants.

Stage 4:

Assume that Equation (17) has the following results:

Case 1: If $\kappa_2 \neq 0$ and $\pi = \kappa_2^2 + 4\kappa_1 - 4\kappa_1\kappa_3 > 0$, then

$$\frac{G'(\eta)}{G(\eta)} = \frac{\kappa_2\sqrt{\pi}\left(C_1 \exp\left(\frac{1}{2}\sqrt{\pi}\eta\right) + C_2 \exp\left(\frac{1}{2}(-\sqrt{\pi})\eta\right)\right)}{(2(1-\kappa_3))\left(C_1 \exp\left(\frac{1}{2}\sqrt{\pi}\eta\right) - C_2 \exp\left(\frac{1}{2}(-\sqrt{\pi})\eta\right)\right)} + \frac{\kappa_2}{2(1-\kappa_3)}. \tag{18}$$

Case 2: If $\kappa_2 \neq 0$ and $\pi = \kappa_2^2 + 4\kappa_1 - 4\kappa_1\kappa_3 < 0$, then

$$\frac{G'(\eta)}{G(\eta)} = \frac{\kappa_2\sqrt{-\pi}(C_1\iota\cos(\frac{1}{2}\sqrt{-\pi}\eta) - C_2\sin(\frac{1}{2}\sqrt{-\pi}\eta))}{(2(1-\kappa_3))(C_1\iota\sin(\frac{1}{2}\sqrt{-\pi}\eta) + C_2\cos(\frac{1}{2}\sqrt{-\pi}\eta))} + \frac{\kappa_2}{2(1-\kappa_3)}. \tag{19}$$

Case 3: If $\kappa_2 = 0$ and $\kappa_1 - \kappa_1\kappa_3 \geq 0$, this provides

$$\frac{G'(\eta)}{G(\eta)} = \frac{\sqrt{\kappa_1 - \kappa_1\kappa_3}(C_2\sin(\eta\sqrt{\kappa_1 - \kappa_1\kappa_3}) + C_1\cos(\eta\sqrt{\kappa_1 - \kappa_1\kappa_3}))}{(1-\kappa_3)(C_1\sin(\eta\sqrt{\kappa_1 - \kappa_1\kappa_3}) - C_2\cos(\eta\sqrt{\kappa_1 - \kappa_1\kappa_3}))}. \tag{20}$$

Case 4: If $\kappa_2 = 0$ and $\kappa_1 - \kappa_1\kappa_3 < 0$, then

$$\frac{G'(\eta)}{G(\eta)} = \frac{\sqrt{\kappa_1\kappa_3 - \kappa_1}(C_1\iota\cosh(\eta\sqrt{\kappa_1\kappa_3 - \kappa_1}) - C_2\sinh(\eta\sqrt{\kappa_1\kappa_3 - \kappa_1}))}{(1-\kappa_3)(C_1\iota\sinh(\eta\sqrt{\kappa_1\kappa_3 - \kappa_1}) - C_2\cosh(\eta\sqrt{\kappa_1\kappa_3 - \kappa_1}))}. \tag{21}$$

here κ_1, κ_2, κ_3, C_1, and C_2 denote the parameters.

Stage 5:

Substitute Equation (16) with Equation (17) in Equation (15) and combine the coefficient of each order of $\left(\frac{G'(\eta)}{G(\eta)}\right)$. Setting them equal to zero, we achieve a set.

Step 6:

Utilize the Mathematica software to solve the gained set of equations.

Step 7:

Using solutions in Equation (16) results in different solitons for Equation (13).

5. Mathematical Analysis

Assuming the following,

$$v(x,t) = V(\zeta), \qquad \zeta = (\frac{1}{\Delta}(x + \frac{1}{\Gamma(\Delta)})^{\Delta} + \lambda\frac{1}{\Delta}(t + \frac{1}{\Gamma(\Delta)})^{\Delta}) \tag{22}$$

using Equation (22) into Equation (2) results in

$$\lambda V' + \mu V'' + VV' = 0. \tag{23}$$

Taking the integration of Equation (23) w.r.t ζ and considering the constant of integration 0 results in the following ODE:

$$\lambda V + \mu V' + \frac{1}{2}V^2 = 0. \tag{24}$$

The value of m is obtained by a homogenous balance approach in Equation (24), and balancing the terms $V^{'}$ and V^2, one obtains $m = 1$.

5.1. Applications of the Extended ShGEE Technique

Equation (6) changes to the given form for $m = 1$:

$$V(\upsilon) = \alpha_0 + \alpha_1\cosh(f(\upsilon)) + \beta_1\sinh(f(\upsilon)). \tag{25}$$

Using Equations (25) and (7) in Equation (24), we gain a system containing α_0, α_1, β_1, λ, and ρ. By manipulation, the results are given in the form of sets.

Set 1:

$$\{\alpha_0 = -\mu, \alpha_1 = -\mu, \beta_1 = -\mu, \lambda = \mu\}. \tag{26}$$

$$v_{11}(x,t) = -\mu(1 \pm \coth(\frac{1}{\Delta}(x + \frac{1}{\Gamma(\Delta)})^{\Delta} + \frac{\mu}{\Delta}(t + \frac{1}{\Gamma(\Delta)})^{\Delta}) \pm \operatorname{csch}(\frac{1}{\Delta}(x + \frac{1}{\Gamma(\Delta)})^{\Delta} + \frac{\mu}{\Delta}(t + \frac{1}{\Gamma(\Delta)})^{\Delta})). \tag{27}$$

$$v_{12}(x,t) = -\mu(1 \pm \tanh(\frac{1}{\Delta}(x+\frac{1}{\Gamma(\Delta)})^{\Delta} + \frac{\mu}{\Delta}(t+\frac{1}{\Gamma(\Delta)})^{\Delta}) \pm \iota\, \mathrm{sech}(\frac{1}{\Delta}(x+\frac{1}{\Gamma(\Delta)})^{\Delta} + \frac{\mu}{\Delta}(t+\frac{1}{\Gamma(\Delta)})^{\Delta})). \quad (28)$$

Set 2:

$$\{\alpha_0 = \mu, \alpha_1 = -\mu, \beta_1 = -\mu, \lambda = -\mu\}. \quad (29)$$

$$v_{21}(x,t) = -\mu(-1 \pm \coth(\frac{1}{\Delta}(x+\frac{1}{\Gamma(\Delta)})^{\Delta} - \frac{\mu}{\Delta}(t+\frac{1}{\Gamma(\Delta)})^{\Delta}) \pm \mathrm{csch}(\frac{1}{\Delta}(x+\frac{1}{\Gamma(\Delta)})^{\Delta} + \lambda\frac{1}{\Delta}(t+\frac{1}{\Gamma(\Delta)})^{\Delta})). \quad (30)$$

$$v_{22}(x,t) = -\mu(-1 \pm \tanh(\frac{1}{\Delta}(x+\frac{1}{\Gamma(\Delta)})^{\Delta} - \frac{\mu}{\Delta}(t+\frac{1}{\Gamma(\Delta)})^{\Delta}) \pm \iota\, \mathrm{sech}(\frac{1}{\Delta}(x+\frac{1}{\Gamma(\Delta)})^{\Delta} + \lambda\frac{1}{\Delta}(t+\frac{1}{\Gamma(\Delta)})^{\Delta})). \quad (31)$$

Set 3:

$$\{\alpha_0 = -\mu, \alpha_1 = -\mu, \beta_1 = \mu, \lambda = \mu\}. \quad (32)$$

$$v_{31}(x,t) = -\mu(1 \pm \coth(\frac{1}{\Delta}(x+\frac{1}{\Gamma(\Delta)})^{\Delta} + \frac{\mu}{\Delta}(t+\frac{1}{\Gamma(\Delta)})^{\Delta}) \mp \mathrm{csch}(\frac{1}{\Delta}(x+\frac{1}{\Gamma(\Delta)})^{\Delta} + \frac{\mu}{\Delta}(t+\frac{1}{\Gamma(\Delta)})^{\Delta})). \quad (33)$$

$$v_{32}(x,t) = -\mu(1 \pm \tanh(\frac{1}{\tau}(x+\frac{1}{\Gamma(\tau)})^{\tau} + \frac{\mu}{\tau}(t+\frac{1}{\Gamma(\tau)})^{\tau}) \mp \iota\, \mathrm{sech}(\frac{1}{\Delta}(x+\frac{1}{\Gamma(\Delta)})^{\Delta} + \frac{\mu}{\Delta}(t+\frac{1}{\Gamma(\Delta)})^{\Delta})). \quad (34)$$

Set 4:

$$\{\alpha_0 = \mu, \alpha_1 = -\mu, \beta_1 = \mu, \lambda = -\mu\}. \quad (35)$$

$$v_{41}(x,t) = \mu(1 \mp \coth(\frac{1}{\Delta}(x+\frac{1}{\Gamma(\Delta)})^{\Delta} - \frac{\mu}{\Delta}(t+\frac{1}{\Gamma(\Delta)})^{\Delta}) \pm \mathrm{csch}(\frac{1}{\Delta}(x+\frac{1}{\Gamma(\Delta)})^{\Delta} - \frac{\mu}{\Delta}(t+\frac{1}{\Gamma(\Delta)})^{\Delta})). \quad (36)$$

$$v_{42}(x,t) = \mu(1 \mp \tanh(\frac{1}{\Delta}(x+\frac{1}{\Gamma(\Delta)})^{\Delta} - \frac{\mu}{\Delta}(t+\frac{1}{\Gamma(\Delta)})^{\Delta}) \pm \iota\, \mathrm{sech}(\frac{1}{\Delta}(x+\frac{1}{\Gamma(\Delta)})^{\Delta} - \frac{\mu}{\Delta}(t+\frac{1}{\Gamma(\Delta)})^{\Delta})). \quad (37)$$

Set 5:

$$\{\alpha_0 = -2\mu, \alpha_1 = -2\mu, \beta_1 = 0, \lambda = 2\mu\}. \quad (38)$$

$$v_{51}(x,t) = -2\mu(1 \pm \coth(\frac{1}{\Delta}(x+\frac{1}{\Gamma(\Delta)})^{\Delta} + \frac{2\mu}{\Delta}(t+\frac{1}{\Gamma(\Delta)})^{\Delta})). \quad (39)$$

$$v_{52}(x,t) = -2\mu(1 \pm \tanh(\frac{1}{\Delta}(x+\frac{1}{\Gamma(\Delta)})^{\Delta} + \frac{2\mu}{\Delta}(t+\frac{1}{\Gamma(\Delta)})^{\Delta})). \quad (40)$$

Set 6:

$$\{\alpha_0 = 2\mu, \alpha_1 = -2\mu, \beta_1 = 0, \lambda = -2\mu\}. \quad (41)$$

$$v_{61}(x,t) = 2\mu(1 \mp \coth(\frac{1}{\Delta}(x+\frac{1}{\Gamma(\Delta)})^{\Delta} - \frac{2\mu}{\Delta}(t+\frac{1}{\Gamma(\Delta)})^{\Delta})). \quad (42)$$

$$v_{62}(x,t) = 2\mu(1 \mp \tanh(\frac{1}{\Delta}(x+\frac{1}{\Gamma(\Delta)})^{\Delta} - \frac{2\mu}{\Delta}(t+\frac{1}{\Gamma(\Delta)})^{\Delta})). \quad (43)$$

5.2. Soliton Solutions via the Improved (G'/G)-Expansion Technique

Equation (16) takes the form for $m = 1$:

$$V(\zeta) = \alpha_0 + \alpha_1\left(\frac{G'(\zeta)}{G(\zeta)}\right). \quad (44)$$

Here, α_0 and α_1 denote undetermined.

Applying Equation (44) with Equation (17) in Equation (24), we achieve the following sets.

Set 1:

$$\left\{\alpha_0 = -\kappa_2\mu - \mu\sqrt{(\kappa_2^2 - 4\kappa_1(\kappa_3 - 1))}, \alpha_1 = -2(\kappa_3 - 1)\mu, \lambda = \mu\sqrt{(\kappa_2^2 - 4\kappa_1(\kappa_3 - 1))}\right\}. \quad (45)$$

Case 1:

$$v(x,t) = -\kappa_2\mu - \mu\sqrt{\kappa_2^2 - 4\kappa_1(\kappa_3-1)} - 2(\kappa_3-1)\mu((\kappa_2\sqrt{\pi}(C_1\exp(\frac{1}{2}(\frac{1}{\Delta}(x+\frac{1}{\Gamma(\Delta)})^\Delta + \frac{\mu\sqrt{\kappa_2^2-4\kappa_1(\kappa_3-1)}}{\Delta}(t+\frac{1}{\Gamma(\Delta)})^\Delta)\sqrt{\pi}) + C_2\exp(\frac{1}{2}(\frac{1}{\Delta}(x+\frac{1}{\Gamma(\Delta)})^\Delta + \frac{\mu\sqrt{\kappa_2^2-4\kappa_1(\kappa_3-1)}}{\Delta}(t+\frac{1}{\Gamma(\Delta)})^\Delta)(-\sqrt{\pi})))/((2(1-\kappa_3))(C_1\exp(\frac{1}{2}(\frac{1}{\Delta}(x+\frac{1}{\Gamma(\Delta)})^\Delta + \frac{\mu\sqrt{(\kappa_2^2-4\kappa_1(\kappa_3-1))}}{\Delta}(t+\frac{1}{\Gamma(\Delta)})^\Delta)\sqrt{\pi}) - C_2\exp(\frac{1}{2}(\frac{1}{\Delta}(x+\frac{1}{\Gamma(\Delta)})^\Delta + \frac{\mu\sqrt{(\kappa_2^2-4\kappa_1(\kappa_3-1))}}{\Delta}(t+\frac{1}{\Gamma(\Delta)})^\Delta)(-\sqrt{\pi}))) + \frac{\kappa_2}{2(1-\kappa_3)}). \quad (46)$$

Case 2:

$$v(x,t) = -\kappa_2\mu - \mu\sqrt{\kappa_2^2 - 4\kappa_1(\kappa_3-1)} - 2(\kappa_3-1)\mu((\kappa_2\sqrt{-\pi}(C_1\iota\cos(\frac{1}{2}(\frac{1}{\Delta}(x+\frac{1}{\Gamma(\Delta)})^\Delta + \frac{\mu\sqrt{\kappa_2^2-4\kappa_1(\kappa_3-1)}}{\Delta}(t+\frac{1}{\Gamma(\Delta)})^\Delta)\sqrt{-\pi}) - C_2\sin(\frac{1}{2}(\frac{1}{\Delta}(x+\frac{1}{\Gamma(\Delta)})^\Delta + \frac{\mu\sqrt{\kappa_2^2-4\kappa_1(\kappa_3-1)}}{\Delta}(t+\frac{1}{\Gamma(\Delta)})^\Delta)\sqrt{-\pi})))/((2(1-\kappa_3))(C_1\iota\sin(\frac{1}{2}(\frac{1}{\Delta}(x+\frac{1}{\Gamma(\Delta)})^\Delta + \frac{\mu\sqrt{(\kappa_2^2-4\kappa_1(\kappa_3-1))}}{\Delta}(t+\frac{1}{\Gamma(\Delta)})^\Delta)\sqrt{-\pi}) + C_2\cos(\frac{1}{2}(\frac{1}{\Delta}(x+\frac{1}{\Gamma(\Delta)})^\Delta + \frac{\mu\sqrt{(\kappa_2^2-4\kappa_1(\kappa_3-1))}}{\Delta}(t+\frac{1}{\Gamma(\Delta)})^\Delta)\sqrt{-\pi}))) + \frac{\kappa_2}{2(1-\kappa_3)}). \quad (47)$$

Case 3:

$$v(x,t) = -\mu\sqrt{-4\kappa_1(\kappa_3-1)} - 2(\kappa_3-1)\mu((\sqrt{\kappa_1-\kappa_1\kappa_3}(C_2\sin((\frac{1}{\Delta}(x+\frac{1}{\Gamma(\Delta)})^\Delta + \frac{\mu\sqrt{-4\kappa_1(\kappa_3-1)}}{\Delta}(t+\frac{1}{\Gamma(\Delta)})^\Delta)\sqrt{\kappa_1-\kappa_1\kappa_3}) + C_1\cos((\frac{1}{\Delta}(x+\frac{1}{\Gamma(\Delta)})^\Delta + \frac{\mu\sqrt{-4\kappa_1(\kappa_3-1)}}{\Delta}(t+\frac{1}{\Gamma(\Delta)})^\Delta)\sqrt{\kappa_1-\kappa_1\kappa_3})))/((1-\kappa_3)(C_1\sin((\frac{1}{\Delta}(x+\frac{1}{\Gamma(\Delta)})^\Delta + \frac{\mu\sqrt{-4\kappa_1(\kappa_3-1)}}{\Delta}(t+\frac{1}{\Gamma(\Delta)})^\Delta)\sqrt{\kappa_1-\kappa_1\kappa_3}) - C_2\cos((\frac{1}{\Delta}(x+\frac{1}{\Gamma(\Delta)})^\Delta + \frac{\mu\sqrt{-4\kappa_1(\kappa_3-1)}}{\Delta}(t+\frac{1}{\Gamma(\Delta)})^\Delta)\sqrt{\kappa_1-\kappa_1\kappa_3}))). \quad (48)$$

Case 4:

$$v(x,t) = -\mu\sqrt{-4\kappa_1(\kappa_3-1)} - 2(\kappa_3-1)\mu((\sqrt{\kappa_1\kappa_3-\kappa_1}(C_1\iota\cosh((\frac{1}{\Delta}(x+\frac{1}{\Gamma(\Delta)})^\Delta + \frac{\mu\sqrt{-4\kappa_1(\kappa_3-1)}}{\Delta}(t+\frac{1}{\Gamma(\Delta)})^\Delta)\sqrt{\kappa_1\kappa_3-\kappa_1}) - C_2\sinh((\frac{1}{\Delta}(x+\frac{1}{\Gamma(\Delta)})^\Delta + \frac{\mu\sqrt{-4\kappa_1(\kappa_3-1)}}{\Delta}(t+\frac{1}{\Gamma(\Delta)})^\Delta)\sqrt{\kappa_1\kappa_3-\kappa_1})))/((1-\kappa_3)(C_1\iota\sinh((\frac{1}{\Delta}(x+\frac{1}{\Gamma(\Delta)})^\Delta + \frac{\mu\sqrt{-4\kappa_1(\kappa_3-1)}}{\Delta}(t+\frac{1}{\Gamma(\Delta)})^\Delta)\sqrt{\kappa_1\kappa_3-\kappa_1}) - C_2\cosh((\frac{1}{\Delta}(x+\frac{1}{\Gamma(\Delta)})^\Delta + \frac{\mu\sqrt{-4\kappa_1(\kappa_3-1)}}{\Delta}(t+\frac{1}{\Gamma(\Delta)})^\Delta)\sqrt{\kappa_1\kappa_3-\kappa_1}))). \quad (49)$$

Set 2:

$$\left\{\alpha_0 = -\kappa_2\mu + \mu\sqrt{(\kappa_2^2-4\kappa_1(\kappa_3-1))}, \alpha_1 = -2(\kappa_3-1)\mu, \lambda = -\mu\sqrt{(\kappa_2^2-4\kappa_1(\kappa_3-1))}\right\}. \quad (50)$$

Case 1:

$$v(x,t) = -\kappa_2\mu + \mu\sqrt{\kappa_2^2 - 4\kappa_1(\kappa_3-1)} - 2(\kappa_3-1)\mu((\kappa_2\sqrt{\pi}(C_1\exp(\frac{1}{2}(\frac{1}{\Delta}(x+\frac{1}{\Gamma(\Delta)})^{\Delta}$$
$$-\frac{\mu\sqrt{\kappa_2^2-4\kappa_1(\kappa_3-1)}}{\Delta}(t+\frac{1}{\Gamma(\Delta)})^{\Delta})\sqrt{\pi}) + C_2\exp(\frac{1}{2}(\frac{1}{\Delta}(x+\frac{1}{\Gamma(\Delta)})^{\Delta} - \frac{\mu\sqrt{\kappa_2^2-4\kappa_1(\kappa_3-1)}}{\Delta}$$
$$(t+\frac{1}{\Gamma(\Delta)})^{\Delta})(-\sqrt{\pi})))) / ((2(1-\kappa_3))(C_1\exp(\frac{1}{2}(\frac{1}{\Delta}(x+\frac{1}{\Gamma(\Delta)})^{\Delta} - \frac{\mu\sqrt{\kappa_2^2-4\kappa_1(\kappa_3-1)}}{\Delta}(t+\frac{1}{\Gamma(\Delta)})^{\Delta})$$
$$\sqrt{\pi}) - C_2\exp(\frac{1}{2}(\frac{1}{\Delta}(x+\frac{1}{\Gamma(\Delta)})^{\Delta} - \frac{\mu\sqrt{(\kappa_2^2-4\kappa_1(\kappa_3-1))}}{\Delta}(t+\frac{1}{\Gamma(\Delta)})^{\Delta})(-\sqrt{\pi})))) + \frac{\kappa_2}{2(1-\kappa_3)}). \quad (51)$$

Case 2:

$$v(x,t) = -\kappa_2\mu + \mu\sqrt{\kappa_2^2 - 4\kappa_1(\kappa_3-1)} - 2(\kappa_3-1)\mu((\kappa_2\sqrt{-\pi}(C_1\iota\cos(\frac{1}{2}(\frac{1}{\Delta}(x+\frac{1}{\Gamma(\Delta)})^{\Delta}$$
$$-\frac{\mu\sqrt{\kappa_2^2-4\kappa_1(\kappa_3-1)}}{\Delta}(t+\frac{1}{\Gamma(\Delta)})^{\Delta})\sqrt{-\pi}) - C_2\sin(\frac{1}{2}(\frac{1}{\Delta}(x+\frac{1}{\Gamma(\Delta)})^{\Delta} - \frac{\mu\sqrt{\kappa_2^2-4\kappa_1(\kappa_3-1)}}{\Delta}$$
$$(t+\frac{1}{\Gamma(\Delta)})^{\Delta})\sqrt{-(\pi)})))) / ((2(1-\kappa_3))(C_1\iota\sin(\frac{1}{2}(\frac{1}{\Delta}(x+\frac{1}{\Gamma(\Delta)})^{\Delta} - \frac{\mu\sqrt{(\kappa_2^2-4\kappa_1(\kappa_3-1))}}{\Delta}(t+\frac{1}{\Gamma(\Delta)})^{\Delta})$$
$$\sqrt{-\pi}) + C_2\cos(\frac{1}{2}(\frac{1}{\Delta}(x+\frac{1}{\Gamma(\Delta)})^{\Delta} - \frac{\mu\sqrt{(\kappa_2^2-4\kappa_1(\kappa_3-1))}}{\Delta}(t+\frac{1}{\Gamma(\Delta)})^{\Delta})\sqrt{-\pi}))) + \frac{\kappa_2}{2(1-\kappa_3)}). \quad (52)$$

Case 3:

$$v(x,t) = \mu\sqrt{4\kappa_1 - 4\kappa_1\kappa_3} - 2(\kappa_3-1)\mu((\sqrt{\kappa_1-\kappa_1\kappa_3}(C_2\sin((\frac{1}{\Delta}(x+\frac{1}{\Gamma(\Delta)})^{\Delta}$$
$$-\frac{\mu\sqrt{4\kappa_1-4\kappa_1\kappa_3}}{\Delta}(t+\frac{1}{\Gamma(\Delta)})^{\Delta})\sqrt{\kappa_1-\kappa_1\kappa_3}) + C_1\cos((\frac{1}{\Delta}(x+\frac{1}{\Gamma(\Delta)})^{\Delta} - \frac{\mu\sqrt{4\kappa_1-4\kappa_1\kappa_3}}{\Delta}$$
$$(t+\frac{1}{\Gamma(\Delta)})^{\Delta})\sqrt{\kappa_1-\kappa_1\kappa_3}))) / ((1-\kappa_3)(C_1\sin((\frac{1}{\Delta}(x+\frac{1}{\Gamma(\Delta)})^{\Delta} - \frac{\mu\sqrt{4\kappa_1-4\kappa_1\kappa_3}}{\Delta}(t+\frac{1}{\Gamma(\Delta)})^{\Delta})$$
$$\sqrt{\kappa_1-\kappa_1\kappa_3}) - C_2\cos((\frac{1}{\Delta}(x+\frac{1}{\Gamma(\Delta)})^{\Delta} - \frac{\mu\sqrt{4\kappa_1-4\kappa_1\kappa_3}}{\Delta}(t+\frac{1}{\Gamma(\Delta)})^{\Delta})\sqrt{\kappa_1-\kappa_1\kappa_3})))). \quad (53)$$

Case 4:

$$v(x,t) = \mu\sqrt{-4\kappa_1(\kappa_3-1)} - 2(\kappa_3-1)\mu((\sqrt{\kappa_1\kappa_3-\kappa_1}(C_1\iota\cosh((\frac{1}{\Delta}(x+\frac{1}{\Gamma(\Delta)})^{\Delta}$$
$$-\frac{\mu\sqrt{-4\kappa_1(\kappa_3-1)}}{\Delta}(t+\frac{1}{\Gamma(\Delta)})^{\Delta})\sqrt{\kappa_1\kappa_3-\kappa_1}) - C_2\sinh((\frac{1}{\Delta}(x+\frac{1}{\Gamma(\Delta)})^{\Delta} - \frac{\mu\sqrt{-4\kappa_1(\kappa_3-1)}}{\Delta}$$
$$(t+\frac{1}{\Gamma(\Delta)})^{\Delta})\sqrt{\kappa_1\kappa_3-\kappa_1}))) / ((1-\kappa_3)(C_1\iota\sinh((\frac{1}{\Delta}(x+\frac{1}{\Gamma(\Delta)})^{\Delta} - \frac{\mu\sqrt{-4\kappa_1(\kappa_3-1)}}{\rho}(t+\frac{1}{\Gamma(\Delta)})^{\Delta})$$
$$\sqrt{\kappa_1\kappa_3-\kappa_1}) - C_2\cosh((\frac{1}{\Delta}(x+\frac{1}{\Gamma(\Delta)})^{\Delta} - \frac{\mu\sqrt{-4\kappa_1(\kappa_3-1)}}{\Delta}(t+\frac{1}{\Gamma(\Delta)})^{\Delta})\sqrt{\kappa_1\kappa_3-\kappa_1})))). \quad (54)$$

6. The Stability Analysis (SA)

Here, we discuss an important analysis of the equation concerned. It is applied for various models, including [37,38]. For Equation (24), the stability analysis, we use the following:

$$\mathcal{S} = \frac{1}{2}\int_{-\infty}^{\infty} v^2\, dx, \tag{55}$$

here, $\mathcal{S}$ represents a factor of momentum and $v(x,t)$ indicates the possibility power. An important criterion of stable solution is shown as

$$\frac{\partial \mathcal{S}}{\partial \lambda} > 0, \tag{56}$$

here, λ denotes a soliton velocity; substituting Equation (31) in Equation (55) yields

$$\mathcal{S} = \frac{1}{2}\int_{-6}^{6} (-\mu(1+\coth(x+\mu t)+\operatorname{csch}(x+\mu t)))^2 dx \tag{57}$$

By using the criterion given in Equation (56), we get the following for $\mu = 0.5$ and $t = 1$:

$$\begin{aligned}
&-\mu^2\Big(\frac{1}{2}t\tanh(3-\frac{\mu t}{2}) - \frac{1}{2}t\coth(\frac{\mu t}{2}+3) - \frac{1}{2}t\coth(3-\frac{\mu t}{2}) - t\coth(\mu t) - t\coth(6-\mu t)\\
&\quad - t\operatorname{csch}^2(\mu t+6) + t\operatorname{csch}^2(6-\mu t) - t\coth(\mu t+6)\operatorname{csch}(\mu t+6) + t\coth(6-\mu t)\operatorname{csch}(6-\mu t)\\
&\quad + \sinh(\mu t+6)\operatorname{csch}(\mu t)\operatorname{sech}(\frac{\mu t}{2}+3)\Big(t\cosh(\frac{\mu t}{2}+3)\cosh(\mu t)\operatorname{csch}(\mu t+6) +\\
&\quad \frac{1}{2}t\sinh(\frac{\mu t}{2}+3)\sinh(\mu t)\operatorname{csch}(\mu t+6) - t\sinh(\mu t)\cosh(\frac{\mu t}{2}+3)\coth(\mu t+6)\operatorname{csch}(\mu t+6)\Big)\Big) > 0.
\end{aligned} \tag{58}$$

Hence, Equation (24) indicates the existence of a stable nonlinear model, provided the condition is fulfilled.

7. The Modulation Instability Analysis

In a nonlinear dispersion medium, a continuous surface wave induces modulation instability, leading to self-modulation of phase and intensity. To achieve the steady-state solution for the Benjamin–Ono model, assume the following relation as in [39]:

$$v(x,t) = \big(\sqrt{\tau} + V(x,t)\big)e^{\iota\tau t} \tag{59}$$

Here, τ indicates the normalized optical power. Using Equation (59) in Equation (1) and by linearizing, we obtain

$$\iota\tau^{3/2} + V_t + \iota\tau V + \mu V_{xx} = 0. \tag{60}$$

Consider the result of Equation (60) given as

$$V(x,t) = A_1 e^{\iota(px-qt)} + A_2 e^{-\iota(px-qt)}. \tag{61}$$

Here, q and p indicate the perturbation frequency and normalization wave number. Inserting Equation (61) in Equation (60) and by collecting each coefficient of $e^{\iota(px-qt)}$ and $e^{-\iota(px-qt)}$, we get a dispersive solution by solving the determinant of the coefficient matrix:

$$\mu^2 p^4 + q^2 - \tau^2 = 0 = 0. \tag{62}$$

Finding the dispersion result of Equation (62) for q yields

$$q = \pm\sqrt{\tau^2 - \mu^2 p^4}. \tag{63}$$

The obtained dispersive result denotes the stable steady state solution. When q is not real, the steady-state result will become unstable due to the steady perturbation increase. When q is real then steady state changes the stable due to decrease in perturbation. A steady-state result will not be stable when

$$\tau^2 - \mu^2 p^4 < 0. \tag{64}$$

The MI gain spectrum $G(p)$ is given as

$$G(p) = 2Im(q) = \sqrt{\tau^2 - \mu^2 p^4}. \tag{65}$$

8. Physical Description

This section explores the physical explanation of solutions derived for a (1+1)-dimensional Benjamin–Ono equation along with a β-time fractional derivative and the previously mentioned methods. To validate the physical accuracy of the mathematical model, we performed visual analyses via 3D plots, density, and 2D illustrations of the solutions. We have also investigated how fractional derivatives and the selected solution methods affect the characteristics and behavior of the solutions. Figure 1 represents the MI gain spectrum of Equation (27) with $\mu = 4$. Figure 2 (singular soliton) shows the 3-D (a), 2-D (b), and contour (c) plots with $\Delta = 0.9$ and $\mu = 0.5$ of $v(x,t)$. Singular soliton is useful in optical physics, fluid dynamics, and mathematical modeling in nonlinear system and dynamics. Figure 3 (dark soliton) shows the 3D (a), 2D (b), and contour (c) plots with $\Delta = 0.1$ and $\mu = 0.5$ of $v(x,t)$ that appear in Equation (28). Dark soliton solutions have applications in optical communications, sensing, nonlinear optics, etc. Figure 4 (rational wave solution) shows the 3D (a), 2D (b), and contour (c) plots with $\Delta = 0.1, \mu = 0.5, \kappa_1 = -0.1, \kappa_2 = 0.2$, $\kappa_3 = 1.5, C_1 = 0.5$, and $C_2 = -0.2$ of $v(x,t)$ which appear in Equation (46). The rational wave solution has applications in nonlinear optics, fluid dynamics, Bose–Einstein condensates, etc. Figure 5 (periodic wave solution) shows the 3D (a), 2D (b), and contour (c) plots with $\Delta = 0.9, \mu = 0.5, \kappa_1 = -0.1, \kappa_2 = 0.2, \kappa_3 = -1.5, C_1 = 0.5$, and $C_2 = -0.2$ of $v(x,t)$ that appear in Equation (47). The periodic wave solution has applications in optical fibers, fluid dynamics, etc. Figure 6 (periodic soliton) shows the 3D (a), 2D (b), and contour (c) plots with $\Delta = 0.9, \mu = 0.5, \kappa_1 = -0.1, \kappa_2 = 0, \kappa_3 = 1.5, C_1 = 0.5$, and $C_2 = -0.2$ of $v(x,t)$ that appear in Equation (48). Figure 7 (kink-singular soliton) shows the 3D(a), 2D(b), and contour(c) plots with $\Delta = 0.1, \mu = 0.5, \kappa_1 = -0.5, \kappa_2 = 0, \kappa_3 = -0.1, C_1 = -0.5$, and $C_2 = 0.2$ of $v(x,t)$ which appear in Equation (49). Kink-singular soliton has applications in nonlinear optics, plasma physics, condensed matter physics, etc.

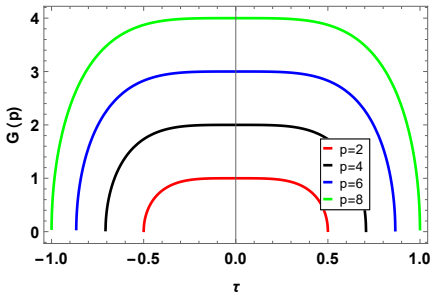

Figure 1. The MI gain spectrum for distinct values of p.

By investigating how fractional orders change the amplitude and phase components, researchers gain crucial information into wave propagation dynamics in harbor and coastal environments. The solitons in fluid dynamics are significant for understanding localized wave phenomena because the dynamics of solitons can mitigate wave energy and the modeling of wave behaviors in marine ecosystems. Some solitons in fluid dynamics have various practical applications and can predict oceanic processes, aiding in the management of offshore activities and marine environments.

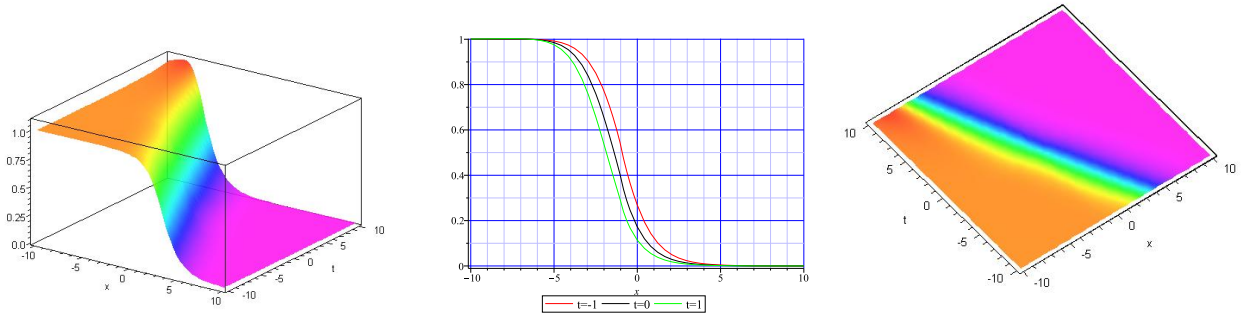

(**a**) (**b**) (**c**)

Figure 2. Physical interpretation of $v(x,t)$ is given in Equation (27). (**a**) represents the 3-D plot, (**b**) shows the 2-D graph at $t=-1,0,1$, and (**c**) represents the contour graph.

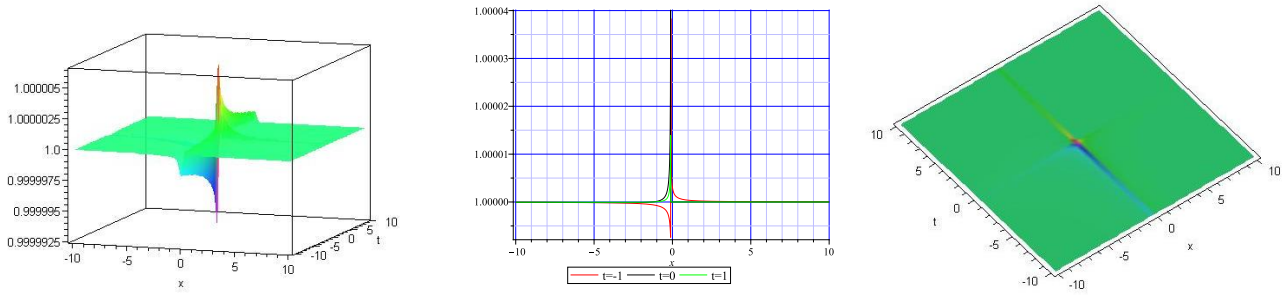

(**a**) (**b**) (**c**)

Figure 3. Physical interpretation of $v(x,t)$, as given in Equation (28). (**a**) represents the 3-D plot, (**b**) shows the 2-D graph at $t=-1,0,1$, and (**c**) represents the contour graph.

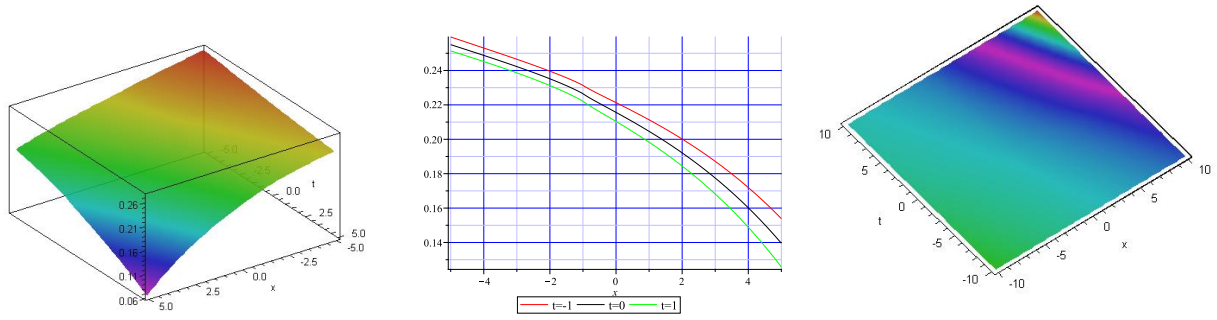

(**a**) (**b**) (**c**)

Figure 4. Graphical interpretation of $v(x,t)$, as shown in Equation (46). (**a**) represents the 3-D plot, (**b**) shows the 2-D graph at $t=-1,0,1$, and (**c**) represents the contour graph.

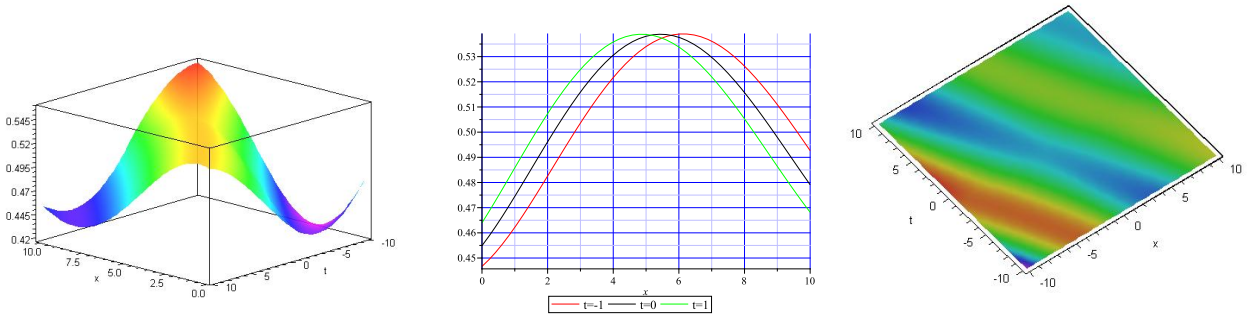

(**a**) (**b**) (**c**)

Figure 5. Graphical interpretation of $v(x,t)$, as shown in Equation (47). (**a**) represents the 3-D plot, (**b**) shows the 2-D graph at $t=-1,0,1$, and (**c**) represents the contour graph.

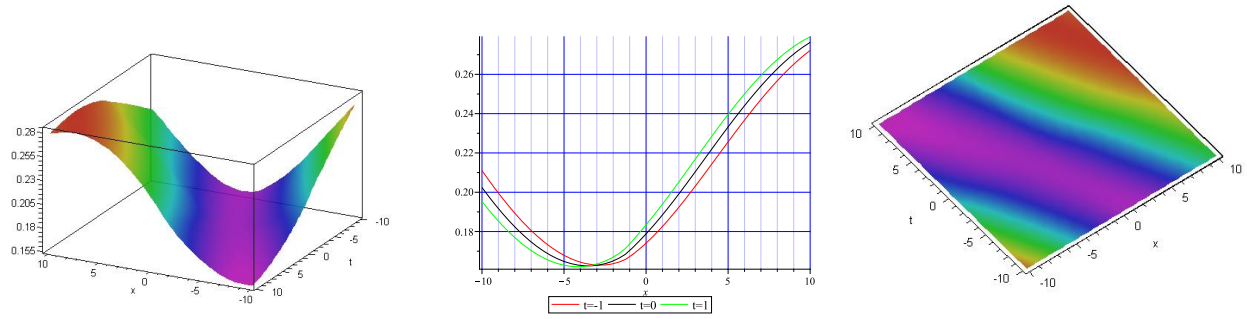

(**a**) (**b**) (**c**)

Figure 6. Graphical interpretation of $v(x,t)$, as shown in Equation (48). (**a**) represents the 3-D plot, (**b**) shows the 2-D graph at $t=-1,0,1$, and (**c**) represents the contour graph.

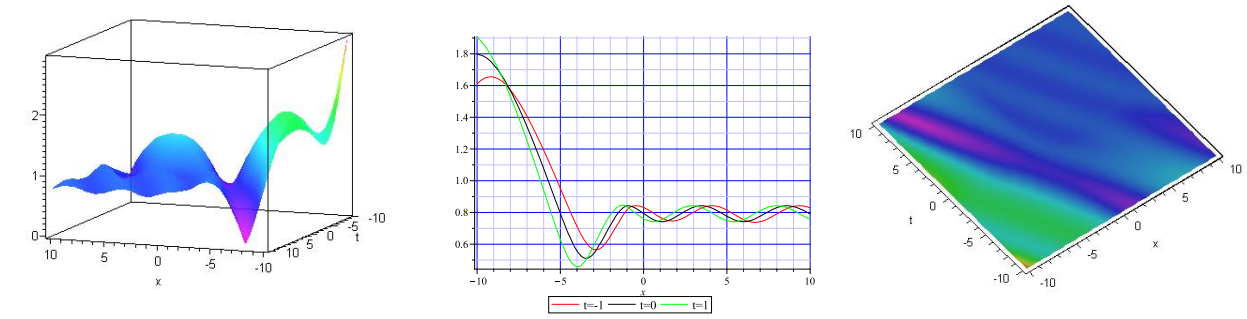

(**a**) (**b**) (**c**)

Figure 7. Graphical interpretation of $v(x,t)$, as shown in Equation (49). (**a**) represents the 3-D plot, (**b**) shows the 2-D graph at $t=-1,0,1$, and (**c**) represents the contour graph.

9. Results and Discussion

In this section, we will compare the existing results and the results obtained in this research. In [25], the extended truncated expansion technique is used to obtain the kink wave solution. In [26], the Jacobi elliptic function expansion scheme is utilized to gain the same traveling wave solutions. In [27], the new generalized (G'/G)-expansion technique is applied to obtain the different traveling soliton solutions. In [29], the (G'/G^2)-expansion method is used to achieve the analytical solutions. Meanwhile, in our research, we utilized the EShGEE technique and the improved (G'/G)-expansion method to obtain the novel

kinds of exact solitons, including periodic, kink, dark, ratonal wave, and kink-singular soliton solutions of the β-time fractional Bejamin-Ono equation.

10. Conclusions

In this study, we have successfully developed a family of novel soliton structures to the Benjamin–Ono equation along beta-time fractional derivative. We obtained the results, achieving singular, singular-bright, dark, singular, singular-dark, kink, and many more solutions with the use of the EShGEE technique and the improved (G'/G)-expansion technique. An effective sense of β-time fractional derivative yields different results compared to the existing results. The Mathematica tool is utilized to achieve as well as verify results. The results are represented by 2-D, 3-D, and contour graphs.

The (1+1)-dimensional nonlinear BO model is an integro-differential equation that explains one-dimensional internal waves in deep water. This equation is used in mathematical physics and dynamics to understand the nature of internal waves in a twin layer fluid. It has many applications in the studies of wave breaking, wave interactions, the evolution of wave patterns, and many more. Furthermore, the stability as well as modulation instability analysis of the concerned equation is also utilized to verify the stability and accuracy of the solutions obtained. Ultimately, the technique we used proved useful for handling NLFPDEs and larger systems of equations. The findings presented here offer substantial insight and potential applications in different scientific and engineering fields.

Author Contributions: Conceptualization, K.U.T.; methodology, M.A.A.; software, K.U.T.; validation, K.U.T.; formal analysis, K.U.T.; investigation, K.U.T.; resources, K.U.T.; writing—original draft preparation, K.U.T.; writing—review and editing, K.U.T.; visualization, M.A.A.; supervision, M.A.A.; project administration, M.A.A.; funding acquisition, M.A.A. All authors have read and agreed to the published version of the manuscript.

Funding: This work was supported by the Deanship of Scientific Research, Vice Presidency for Graduate Studies and Scientific Research, King Faisal University, Saudi Arabia [Grant No. KFU251047].

Data Availability Statement: Data sharing is not applicable to this article as no datasets were generated or analyzed during this study.

Conflicts of Interest: The authors declare no conflicts of interest.

References

1. Razzaq, W.; Zafar, A.; Raheel, M. Searching the new exact wave solutions to the beta-fractional Paraxial nonlinear Schrödinger model via three different approaches. *Int. J. Mod. Phys. B* **2024**, *38*, 2450132. [CrossRef]
2. Qawaqneh, H.; Zafar, A.; Raheel, M.; Zaagan, A.A.; Zahran, E.H.; Cevikel, A.; Bekir, A. New soliton solutions of M-fractional Westervelt model in ultrasound imaging via two analytical techniques. *Opt. Quantum Electron.* **2024**, *56*, 737. [CrossRef]
3. Khater, M.M.A. Novel constructed dark, bright and rogue waves of three models of the well-known nonlinear Schrödinger equation. *Int. J. Mod. Phys. B* **2024**, *38*, 2450023. [CrossRef]
4. Khater, M.M.A. Exploring the rich solution landscape of the generalized Kawahara equation: Insights from analytical techniques. *Eur. Phys. J. Plus* **2024**, *139*, 184. [CrossRef]
5. Walait, A.; Ashraf, H.; Chou, D.; Rehman, H.U. Stagnant Rings and Uniform Film Analysis of Phan-Thien Tanner Fluid Film Flow on a Vertically Upward Moving Tube. *Phys. Fluids* **2024**, *36*, 083613. [CrossRef]
6. Khater, M.M.A. Comment on the paper of El-Ganaini et al. [Chaos, Solitons and Fractals 140 (2020) 110218]. *Chaos Solitons Fractals* **2024**, *182*, 114729. [CrossRef]
7. Bezgabadi, A.S.; Bolorizadeh, M.A. Analytic combined bright-dark, bright and dark solitons solutions of generalized nonlinear Schrödinger equation using extended sinh-Gordon equation expansion method. *Results Phys.* **2021**, *30*, 104852. [CrossRef]
8. Kumar, D.; Manafian, J.; Hawlader, F.; Ranjbaran, A. New closed form soliton and other solutions of the Kundu–Eckhaus equation via the extended sinh-Gordon equation expansion method. *Optik* **2018**, *160*, 159–167. [CrossRef]
9. Ilhan, O.A.; Manafian, J. Analytical treatment in optical metamaterials with anti-cubic law of nonlinearity by improved exp (-Ω (η))-expansion method and extended sinh-Gordon equation expansion method. *Rev. Mex. Física* **2019**, *65*, 658–677. [CrossRef]

10. Qawaqneh, H.; Hakami, K.H.; Altalbe, A.; Bayram, M. The Discovery of Truncated M-Fractional Exact Solitons and a Qualitative Analysis of the Generalized Bretherton Model. *Mathematics* **2024**, *12*, 2772. [CrossRef]
11. Zayed EM, E.; Al-Joudi, S. Applications of an Improved (G'/G)-expansion Method to Nonlinear PDEs in Mathematical Physics. In *AIP Conference Proceedings*; American Institute of Physics: College Park, MD, USA, 2009; Volume 1168, pp. 371–376.
12. Sahoo, S.; Ray, S.S.; Abdou, M.A. New exact solutions for time-fractional Kaup–Kupershmidt equation using improved (G'/G)-expansion and extended (G'/G)-expansion methods. *Alex. Eng. J.* **2020**, *59*, 3105–3110. [CrossRef]
13. Zayed, E.M.E. A further improved (g'/g)-expansion method and the extended tanh-method for finding exact solutions of nonlinear pdes. *Wseas Trans. Math.* **2011**, *10*, 56–64.
14. Qawaqneh, H.; Alrashedi, Y. Mathematical and Physical Analysis of Fractional Estevez–Mansfield–Clarkson Equation. *Fractal Fract.* **2024**, *8*, 467. [CrossRef]
15. Alhefthi, R.K.; Tariq, K.U.; Wazwaz, A.M.; Mehboob, F. On the nonlinear wave structures and stability analysis for the new generalized stochastic fractional potential-kdv model in dispersive medium. *Opt. Quantum Electron.* **2024**, *56*, 662. [CrossRef]
16. Abdeljawad, T. On conformable fractional calculus. *J. Comput. Appl. Math.* **2015**, *279*, 57–66. [CrossRef]
17. Tariq, K.U.; Khater, M.M.; Ilyas, M.; Rezazadeh, H.; Inc, M. Soliton structures for a generalized unstable space-time fractional nonlinear Schrödinger model in mathematical physics. *Int. J. Mod. Phys. B* **2024**, *38*, 2450174. [CrossRef]
18. Wu, G.-Z.; Yu, L.J.; Wang, Y.Y. Fractional optical solitons of the spacetime fractional nonlinear Schrödinger equation. *Optik* **2020**, *207*, 164405. [CrossRef]
19. Almeida, R. A caputo fractional derivative of a function with respect to another function. *Commun. Nonlinear Sci. Numer. Simul.* **2017**, *44*, 460–481. [CrossRef]
20. Jumarie, G. Modified riemann-liouville derivative and fractional taylor series of nondifferentiable functions further results. *Comput. Math. Appl.* **2006**, *51*, 1367–1376. [CrossRef]
21. Gurefe, Y. The generalized kudryashov method for the nonlinear fractional partial differential equations with the beta-derivative. *Rev. Mex. Fis.* **2020**, *66*, 771–781. [CrossRef]
22. Atangana, A.; Baleanu, D.; Alsaedi, A. Analysis of time-fractional Hunter–Saxton equation: A model of neumatic liquid crystal. *Open Phys.* **2016**, *14*, 145–149. [CrossRef]
23. Uddin, M.F.; Hafez, M.G.; Hammouch, Z.; Baleanu, D. Periodic and rogue waves for Heisenberg models of ferromagnetic spin chains with fractional beta derivative evolution and obliqueness. *Waves Random Complex Media* **2020**, *31*, 2135–2149. [CrossRef]
24. Ghanbari, B.; Gómez-Aguilar, J.F. The generalized exponential rational function method for Radhakrishnan–Kundu–Lakshmanan equation with Beta time derivative. *Rev. Mex. Física* **2019**, *65*, 503–518. [CrossRef]
25. Khater, M.M.; Muhammad, S.; Al-Ghamdi, A.; Higazy, M. Abundant wave structures of the fractional Benjamin-Ono equation through two computational techniques. *J. Ocean. Eng. Sci.* 2022, *in press*.
26. Tasbozan, O. New analytical solutions for time fractional Benjamin-Ono equation arising internal waves in deep water. *China Ocean. Eng.* **2019**, *33*, 593–600. [CrossRef]
27. Alam, M.N.; Akbar, M.A. Traveling wave solutions of nonlinear evolution equations via the new generalized (G'/G)-expansion method. *Univers. J. Comput. Math.* **2013**, *1*, 129–136. [CrossRef]
28. Islam, R.; Alam, M.N.; Hossain, A.K.M.K.S.; Roshid, H.O.; Akbar, M.A. Traveling wave solutions of nonlinear evolution equations via $\exp(-\Phi(\eta))$-expansion method. *Glob. J. Sci. Front. Res.* **2013**, *13*, 63–71.
29. Aderyani, S.R.; Saadati, R.; Vahidi, J. Multiple exp-function method to solve the nonlinear space–time fractional partial differential symmetric regularized long wave (SRLW) equation and the (1+1)-dimensional Benjamin–Ono equation. *Int. J. Mod. Phys. B* **2023**, *37*, 2350213. [CrossRef]
30. Karaman B. The use of improved-F expansion method for the time-fractional Benjamin–Ono equation. *Revista de la Real Academia de Ciencias Exactas, Físicas y Naturales. Serie A. Matemáticas* **2021**, *115*, 128. [CrossRef]
31. Alizadeh, F.; Hashemi, M.S.; Haji Badali, A. Lie symmetries, exact solutions, and conservation laws of the nonlinear time-fractional Benjamin-Ono equation. Comput. *Methods Differ. Equ.* **2022**, *10*, 608–616.
32. Sagar, B.; Ray, S.S. A localized meshfree technique for solving fractional Benjamin–Ono equation describing long internal waves in deep stratified fluids. Commun. *Nonlinear Sci. Numer. Simul.* **2023**, *123*, 107287. [CrossRef]
33. Babajanov, B.; Abdikarimov, F. Soliton and periodic wave solutions of the nonlinear loaded (3+1)-dimensional version of the benjamin-ono equation by functional variable method. *J. Nonlinear Model. Anal.* **2023**, *5*, 782–789.
34. Yang, H.; Sun, J.; Fu, C. Time-fractional Benjamin-Ono equation for algebraic gravity solitary waves in baroclinic atmosphere and exact multi-soliton solution as well as interaction. Commun. *Nonlinear Sci. Numer. Simul.* **2019**, *71*, 187–201. [CrossRef]
35. Yang, X.L.; Tang, J.S. Travelling wave solutions for Konopelchenko-Dubrovsky equation using an extended sinh-Gordon equation expansion method. *Commun. Theor. Phys.* **2008**, *50*, 10471051.
36. Tariq, K.U.; Bekir, A.; Nisar, S. The dynamical structures of the Sharma–Tasso–Olver model in doubly dispersive medium. *Chaos Solitons Fractals* **2023**, *177*, 114290. [CrossRef]

37. Tariq, K.U.; Wazwaz, A.M.; Javed, R. Construction of different wave structures, stability analysis and modulation instability of the coupled nonlinear Drinfel'd-Sokolov-Wilson model. *Chaos Solitons Fractals* **2023**, *166*, 112903. [CrossRef]
38. Zulfiqar, H.; Aashiq, A.; Tariq, K.U.; Ahmad, H.; Almohsen, B.; Aslam, M.; Rehman, H.U. On the solitonic wave structures and stability analysis of the stochastic nonlinear Schrödinger equation with the impact of multiplicative noise. *Optik* **2023**, *289*, 171250. [CrossRef]
39. ur Rehman, S.; Ahmad, J. Modulation instability analysis and optical solitons in birefringent fibers to RKL equation without four wave mixing. *Alex. Eng. J.* **2021**, *60*, 1339–1354. [CrossRef]

Disclaimer/Publisher's Note: The statements, opinions and data contained in all publications are solely those of the individual author(s) and contributor(s) and not of MDPI and/or the editor(s). MDPI and/or the editor(s) disclaim responsibility for any injury to people or property resulting from any ideas, methods, instructions or products referred to in the content.